



# Analyzing sandwich panel with new proposed core for bending and compression resistance

Tarek Mesto, Maya Sleiman, Khaled Khalil, Samer Alfayad, Frédéric Jacquemin

## ► To cite this version:

Tarek Mesto, Maya Sleiman, Khaled Khalil, Samer Alfayad, Frédéric Jacquemin. Analyzing sandwich panel with new proposed core for bending and compression resistance. Proceedings of the Institution of Mechanical Engineers, Part L: Journal of Materials: Design and Applications, 2023, 237 (2), pp.367–378. 10.1177/14644207221115576 . hal-03741376

**HAL Id: hal-03741376**

**<https://univ-evry.hal.science/hal-03741376>**

Submitted on 29 Sep 2022

**HAL** is a multi-disciplinary open access archive for the deposit and dissemination of scientific research documents, whether they are published or not. The documents may come from teaching and research institutions in France or abroad, or from public or private research centers.

L'archive ouverte pluridisciplinaire **HAL**, est destinée au dépôt et à la diffusion de documents scientifiques de niveau recherche, publiés ou non, émanant des établissements d'enseignement et de recherche français ou étrangers, des laboratoires publics ou privés.

# Analyzing sandwich panel with new proposed core for bending and compression resistance

Tarek Mesto<sup>1</sup>, Maya Sleiman<sup>2</sup>, Khaled Khalil<sup>1,3</sup> , Samer Alfayad<sup>2</sup> and Frédéric Jacquemin<sup>4</sup>

## Abstract

Sandwich panels are used in many industries for their lightweight compared to high strength. Most of the sandwich panels application are bending and compression, which relies on the core type of the panel. Widely used in additive manufacturing is pyramid cell cores. In this article, two new cores, the reinforced pyramid cell model and the C-half circle cell model, are proposed to replace the pyramidal core and to verify their advantages and disadvantages with respect to it compression and in bending. The comparison was done in the ABAQUS simulation. A semi-analytical method was used as well as experimental tests were carried out to verify the numerical simulation on ABAQUS. The results have been validated, the difference remains below 10%. According to the simulations, the deformation of the skin of the half circle cell panel decreases by 15% in compression while the deflection of the reinforced pyramid cell panel decreases by 26% in bending compared to the pyramid cell panel. However, the most effective results in absorbing compression are half circle cell which is allowed to make impact insulation.

## Keywords

Sandwich panel, lattice core, three-dimensional printing, bending test, compression test, homogenization

## Introduction

With the increasing of many industries, such as automotive, aerospace, marine, and others, energy reduction is needed, thus the weight of the material with the same strength shall be decreased. This is the main function of a sandwich panel, that it replaces a specific part with the same strength and lower weight, insulation, and acoustic insulation.<sup>1,2</sup>

In the classical sandwich panel, the core was filled with foam used to insulate the sandwich panel its thickness. As the industries needed the light-weight material with more strength, they started to make them with a shaped core. The classical sandwich panels were corrugated of other shapes that have one is high strength in one direction but in the other direction is a weak axis.<sup>3,4</sup>

A more recent sandwich core is made from two-dimensional (2D) and three-dimensional (3D) lattice shapes which have a structural repetitive geometry in both directions the width and height.<sup>5</sup> The difference between the 2D and 3D lattice is that the section along the depth of the sandwich panel is the same in 2D and varies in 3D. The 2D lattice, like a honeycomb, has a 2D geometry that is extruded to the thickness of the panel.<sup>5</sup> The 3D shape, like a pyramid, has a 3D object also patterns through the panel.<sup>6</sup>

These sandwich panels are nowadays an essential part in most of applications, so the design and fabrication shall be fast and easy and has a fast process. For that with the complex 3D shape pattern of the core, the design and calculation are high cost and time. A method to reduce time cost is to transform this complex geometry into an orthotropic plate to easily calculate the bending deflection and other uses such as acoustic and thermal insulation have been verified for several shapes.<sup>7</sup> Some of the shapes have been optimized for the sandwich panel as diamond prismatic core (with corrugation order 4) is weigh efficient than trusses when is optimized to a given load in a certain direction Valdevit et al.<sup>8</sup>

---

<sup>1</sup>Faculty of Engineering, CRSI, MMC Laboratory, Lebanese University, Beirut, Lebanon

<sup>2</sup>IBISC Laboratory, University of Evry Val d'Essonne, University Paris-Saclay, Evry, France

<sup>3</sup>ECAM-Rennes, Campus de Ker-Lann, 2 Ctr Antoine de Saint-Exupéry, Bruz, France

<sup>4</sup>Université de Nantes, Institut GeM, UMR CNRS 6183, Equipe E3M, Saint-Nazaire, France

A more complex shape has been added as a lattice core that is fabricated exclusively by additive manufacturing which is time and cost consumption. Work has been done to give high strength and absorb energy. Unit cell analyses show these novel lattices with embedding different ribs into a classic re-entrant structure, have significantly increased Young's modulus along the loading direction.<sup>9,10</sup> Other analysis of the mechanical behavior of octet-truss microstructures has been done experimentally and numerically. The result can be considered a promising structure for printing in the field of tissue engineering.<sup>10</sup> A review of six-lattice Kagome geometry, as an ABS material, has been analyzed experimentally and numerically. Both numerical and experimental approaches were used to evaluate the flexural properties and failure behavior of the sandwich structures under three-point bending tests.<sup>5</sup>

Other than the complex 3D shapes that need 3D printing to be fabricated, a set of modified pyramids and a set of cores are to be compared to the original pyramid core, for compression and bending experiments. In this work, the simulation will be done ABAQUS for bending of

analytical solution of the unit cell response under complex loading.<sup>13</sup> The work derives analytical solutions for the same homogenized method and compares it experimentally and analytically. The results comparison was high accuracy between both and in the semi-analytical has less time of computing.

Initially, the numerical model is validated on ABAQUS by a semi-analytical comparison on steel pyramid cell (PC) core panels.

### Homogenization pyramid lattice core

The homogenization equation of the pyramid lattice core sandwich is done by Liu et al.<sup>11,12</sup> The homogenization was done assuming the rods of the cell are Euler-Bernoulli beams and the equation are done if the material in the elastic region, the rods per thickness of core is  $< 10\%$   $r/h < 0.1$ .

The " $C^H$ " coefficient is the effective stiffness of the homogenized pyramid core, the exact analytical solution of the PC is given by<sup>11</sup>

$$C^H = \frac{157r_c^2 E}{200 \left( \frac{1}{2} D^2 + h_c^2 \right)^{3/2} h_c} \begin{bmatrix} D^2 & D^2 & 0 & 0 & 0 & 0 \\ 0 & D^2 & 4hc_c^2 & 0 & 0 & 0 \\ 0 & 0 & 16h_c^4 / D^2 & 0 & 0 & 0 \\ 0 & 0 & 0 & 4h_c^2 & 0 & 0 \\ 0 & 0 & 0 & 0 & 4h_c^2 & 0 \\ 0 & 0 & 0 & 0 & 0 & D^2 \end{bmatrix} + \frac{r_c^4 E}{(2D^2 + 4h_c^2)^{5/2} h_c} \begin{bmatrix} DD_1 & -75.9D^2 & -301.59h_c^2 & 0 & 0 & 0 \\ -75.9D^2 & D^2 & -301.59h_c^2 & 0 & 0 & 0 \\ -301.59h_c^2 & -301.59h_c^2 & 603.2h_c^2 & 0 & 0 & 0 \\ 0 & 0 & 0 & DD_2 & 0 & 0 \\ 0 & 0 & 0 & 0 & DD_2 & 0 \\ 0 & 0 & 0 & 0 & 0 & 150.8h^2 \end{bmatrix}$$

the pyramid shape by analytical and experimental results. As soon as the numerical simulation is verified, the work is continued on ABAQUS to compare the new set of 3D cores.

### Analytical verification

More shapes have been investigated to obtain analytically the elastic constant by Liu et al.<sup>11,12</sup> for pyramid, tetra, and Kagome core, the work is obtaining an analytical equation from the shape parameters for homogenization of the geometric core as an orthotropic plate, this was to assume that the rod is Euler-Bernoulli beams. The same steps and assumption for homogenization of triangle core have been derived.<sup>11,12</sup>

Another side has been working on the Bernoulli-Euler and Timoshenko beam theories that are used for the

or  $E$  is Young's modulus,  $D$  is the width of the cell,  $h_c$  is the height of the core,  $r_c$  is the radius of the rod,  $DD_1 = 75.9(4 \cdot h_c^2 + D^2)$ ,  $DD_2 = 301.59h_c^4 - 75.4h_c^2 D^2 + 37.7D^4 / D^2$ .

The sandwich now can be expressed as three orthotropic plates as shown in Figure 1 as the two skins and the homogenized core. The three plates of the sandwich panel can be homogenized into one orthotropic plate by the laminate theory to obtain the equivalent elastic constants (Figure 2).

### Numerical modeling

The size of the panels shall comply with the standard code of sandwich panel "ASTMD7249," for using the 3-point bending test. The size for all sandwich panels shall be 500 mm in length, 40 mm in thick, and 100 mm in width, which is more than two times the thickness of the core. The thickness of the skin is 3.3 mm.

The diameter of the rod  $\leq 0.1 h_c$ , where  $h_c$  is the thickness of the core and the cell width is  $D=20$  mm with a ratio of  $w/C=0.5$ . The material of testing in the model between 3D and orthotropic is steel with modulus of elasticity  $E=206$  GPa, Poisson ratio  $\nu = 0.3$ , and density  $\rho = 7850$  kg/m<sup>3</sup>.

The mesh data was taken as element size of 1 mm for the skin and 0.57 mm for the rod and type C3D8R: an 8-node linear brick, reduced integration, and hourglass control. The boundary conditions are the same as the experimental and semi-analytical, which are placed freely on the supports.

Table 1 shows the specification of the sandwich panel with pyramid core, and the equivalent homogenized orthotropic plate. Note that material-1 is the equivalent elastic constant of the pyramid sandwich panel with steel material.

## Results and discussions

The simulation check for the real and analytical shape 3-point bending test was carried out as follows. The 3-point bending test will be simulated on ABAQUS for



**Figure 1.** Sandwich panel with pyramid lattice core.

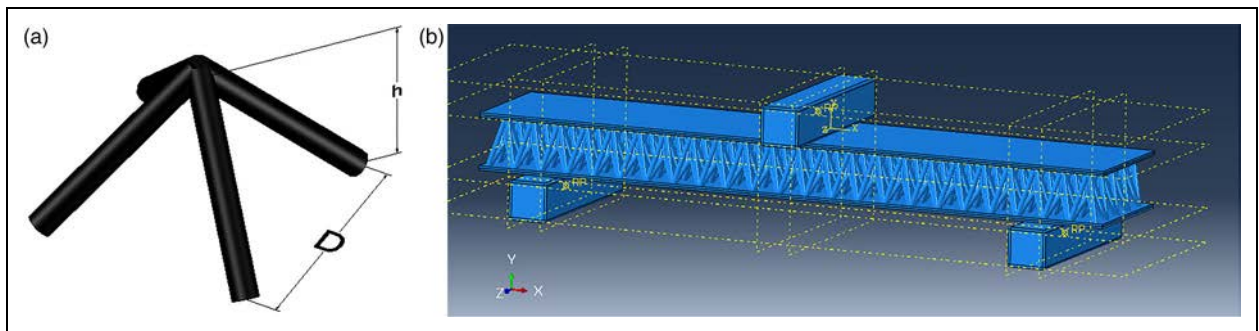


**Figure 2.** Sandwich panel with pyramid core: (a) pyramid cell and (b) panel under bending test model.

**Table 1.** Material properties for the sandwich panel.

	Thickness (mm)	Cell number	Cell width (mm)	Section type	Section size (mm)	Material type
Upper and lower skin	3.3	N/A	N/A	N/A	N/A	Steel
Pyramid core	40	25 × 5	20	Circular rod	4	Steel

the 3D pyramidal core, and also for the equivalent homogenized orthotropic plate. The data of the orthotropic plate are calculated according to equation (1).

Using python script, the equivalent material data of orthotropic plate are given as “Material-1,”  $E_1 = 29.25$  GPa,  $E_2 = 29.2$  GPa,  $G_{12} = 11.2$  GPa, and  $\nu_{12} = 0.29$ .

The dimensions of the plate are the same as given in Table 1. The results of the reaction, obtained by the simulation and by the semi-analytical model are shown in Figure 3.

It is noticed that the results obtained by the numerical model and by the semi-analytical model are very close and begin to diverge when the force increases therefore the deflection increases for a deflection less than 1 mm, the difference between the digital model and the analytical model is less than 10%.

## Experimental verification

After having validated the numerical model in a semi-analytical way, it will be compared with experimental results. For technical reasons, it cannot produce steel PC panels, but they are manufactured by 3D printing of acrylonitrile butadiene styrene (ABS) panels to validate the digital model on ABAQUS.

## Material specification

The ABS mechanical properties vary with the small variation of temperature and can be affected by the temperature of the printing head. To check the repeatability of the results, five ABS samples are fabricated on a 3D printer under the same conditions. The tensile test is carried out on specimens according to the standard ISO-527-2T-1A at a speed of 2 mm/min until rupture in the machine model MTS 20/M (Figure 4). The test was to obtain the stress–strain relationship curve to calculate

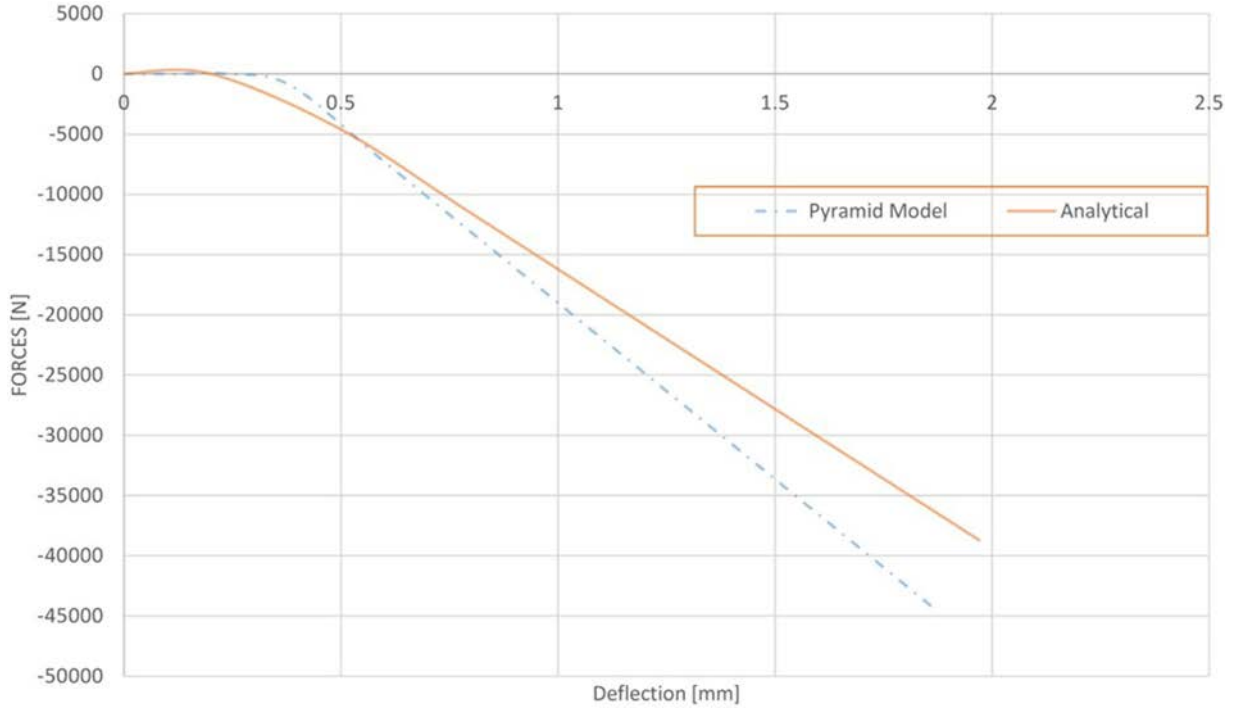


**Figure 3.** The plot of bending results between real model and analytical model of sandwich panel.



**Figure 4.** The sample under tensile test.

the equivalent modulus of elasticity of ABS. From the curve (Figure 5), the modulus of elasticity is obtained from the slope of the stress–strain curve. It is found from the curve that the value of  $E=2.1$  GPa for the ABS obtained by 3D impression, which is near to the commercial values of the material (Figures 6 and 7).

### **Bending test**

After the traction test of the specimens to obtain the ABS mechanical properties, the bending test is made of the Sandwich panel with a pyramid core. The sandwich panel with pyramid cores was modeled in ABAQUS and then exported to an STL file to be 3D printed so that the simulation model and the actual test model were the same size and geometry. The geometry of the specimen is the same high as numerical verification and the same width cell size, but due to the limit of the machine, the width of the specimen is 45 mm and the length is 255 mm.

The machine used is “MTS Capteur DM22,” the radius of the supports is 10 mm and the span between the supports is 200 mm with a speed of 6 mm/min. Three tests were done for the three specimens until they cracked to obtain the force–displacement and time of each experiment. The three tests of the sandwich panel have given the same results about the maximum force of  $F=1200$  N and max displacement at that force of  $d=4.6$  mm into the panel until they are cracked as shown in Figure 8. It is noticed that the rupture occurs systematically at the interface between the top of the pyramid and the skin.

The same model that was created in ABAQUS. The radius of the supports and the span were the same 10 and 200 mm, respectively. The material was defined as 3D body and mechanical properties according to data from the tensile test. The mesh data was taken as element size of 1 mm for the skin and 0.57 mm for the rod and type C3D8R: An 8-node linear brick, reduced integration, and hourglass control. Figure 9 shows the results obtained by

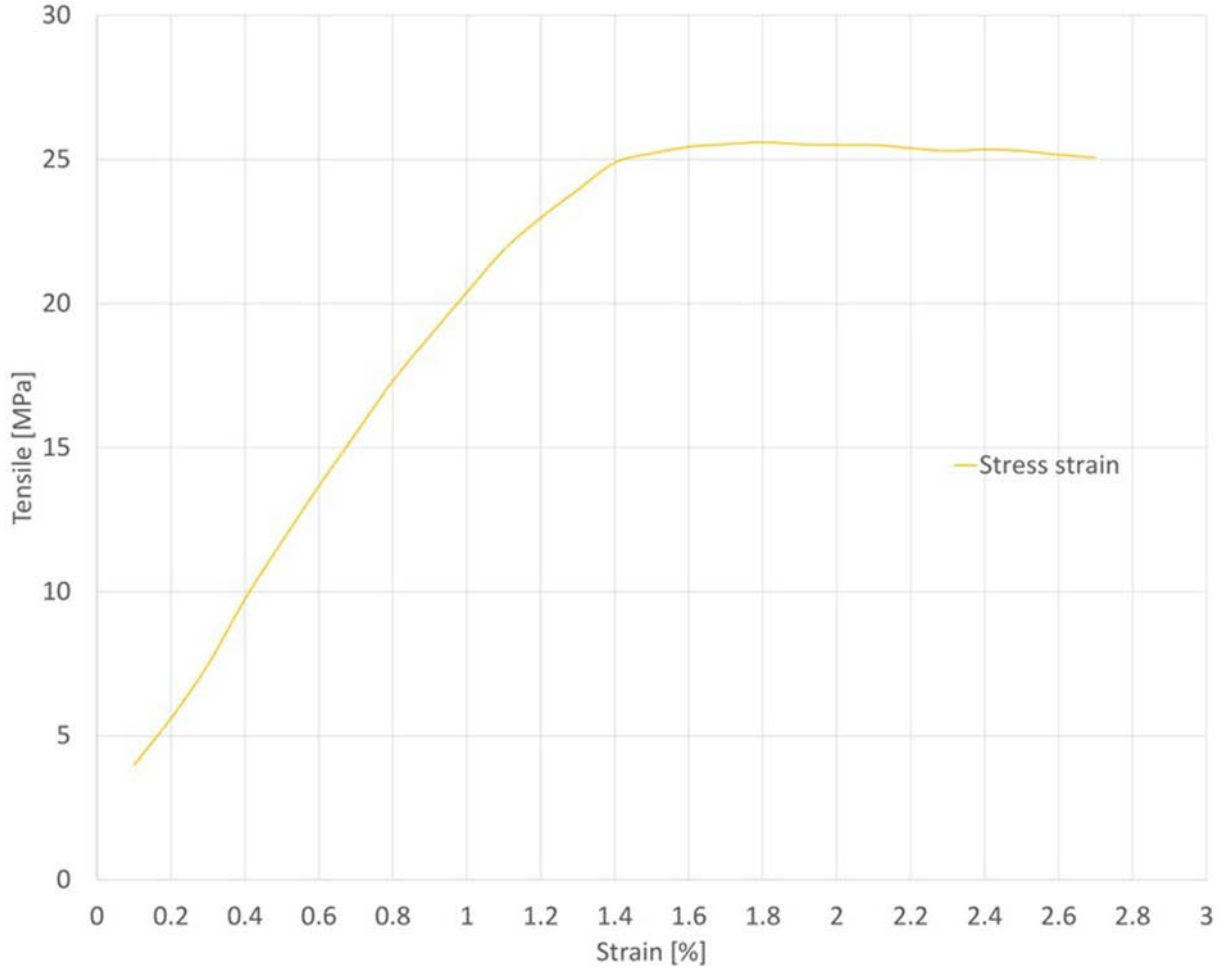


**Figure 5.** Tensile test stress–strain curve.

simulation and by experimental tests by a bending test. The results show that for a deflection  $< 0.5$  mm, the results of the simulation on ABAQUS are very close to those given by the experimental test, the difference is  $< 10\%$ . For larger forces and therefore larger deflections, the difference between the two increases and therefore it is suspected that the material is outside its elastic range. Table 2 has some values for the difference found between the two approaches.

### New lattice shapes

The numerical model is validated on ABAQUS analytically and experimentally and therefore the behavior can be simulated of new lattice core forms to express their advantages and disadvantages compared to the pyramidal model PC in compression and bending.

### Proposed shapes

Many models have been used as a 3D lattice core made from circular rods, pyramid, tetra core, and others which can be manufactured by additive manufacturing. Two shapes, in addition to PC, are introduced as shown in

Figure 4, which will be studied and compared to the classical pyramid.

A reinforced pyramid cell (RPC) shape core consists of a normal pyramid made of four rods and a small pyramid that both are connected with a small rod in the middle. All the rods have the same diameter  $r_d$ .

The half circle cell (HCC) shape core consists of four circles connected at its center; all the circles are bent rods with the same diameter as the pyramid rods. The sandwich panel is two skins and a shaped core, the dimension of all the panels for the experiment are the same size given before.

### Numerical modeling

The simulation of the 3-point bending test, using ABAQUS, will study the three new shapes that have the same dimensions as the verification test that comply with the standards. The dimensions of the panels are  $500 \text{ mm} \times 100 \text{ mm} \times 40 \text{ mm}$  core thick. The pattern is  $23 \text{ cell} \times 9 \text{ cell}$  width. The radius of the rod is assumed an Euler-Keppler beam which has a ratio radius/length is  $< 0.1$ .<sup>3</sup>

The numerical simulation for the three sandwich panels is done to check the resistance of the bending





**Figure 6.** Experimental bending test.

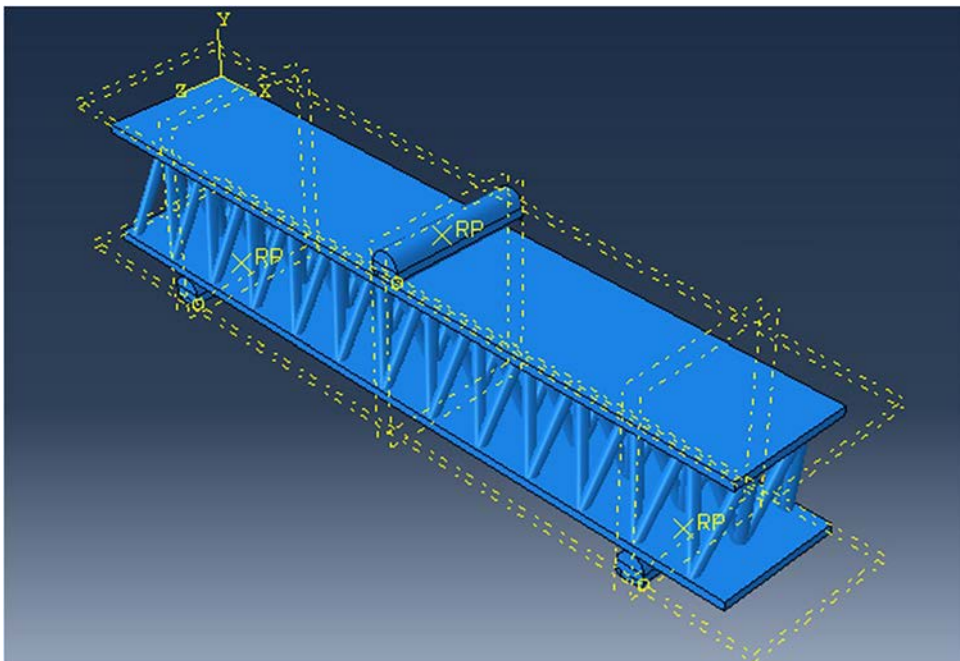


**Figure 7.** Simulation verification of the same panel of experimental tests.



**Figure 8.** Rupture aspect for the pyramid core sandwich panel.

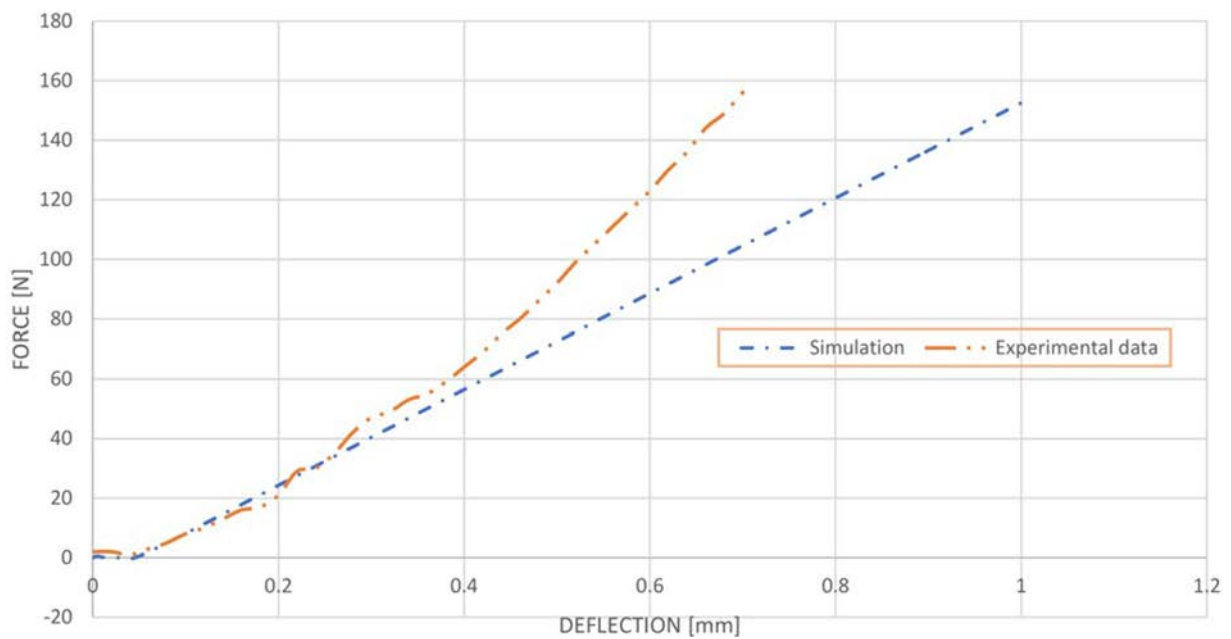


**Figure 9.** Comparison of the three experiences with the numerical simulation.

load of each core. The support and bending block are assumed as rigid bodies. The skins are modeled as shells and the rods of the shapes are modeled as wires. The ABS, density =  $1060 \text{ kg/m}^3$  and Young's modulus =  $2.1 \text{ GPa}$ , is used as a material for both the skins and core.

The skin and the shaped rod are assembled in the drawing, and the core is attached as a "tie constraint" with the upper and lower skin. The mesh of the rod is set to be 1 mm elements and type of "A 2-node linear beam in space." For the skin, as a shell, the size of the element is also taken as  $5 \text{ mm} \times 5 \text{ mm}$ , and the type "S4R-A 4-node doubly curved thin shell, reduced integration, hourglass control, finite membrane strains."

The boundary condition is fixed with the horizontal direction free to move, and this condition is set to the

**Table 2.** Difference between simulation and experimental of Figure 9.

Deflection (mm)	Simulation force (N)	Experience force (N)	% diff.
0.09	7.24	7.5	3.50
0.17	20.17	18.5	9.01
0.29	39.53	42.0	5.89
0.47	68.50	75.0	8.67
0.69	102.35	123.0	16.79



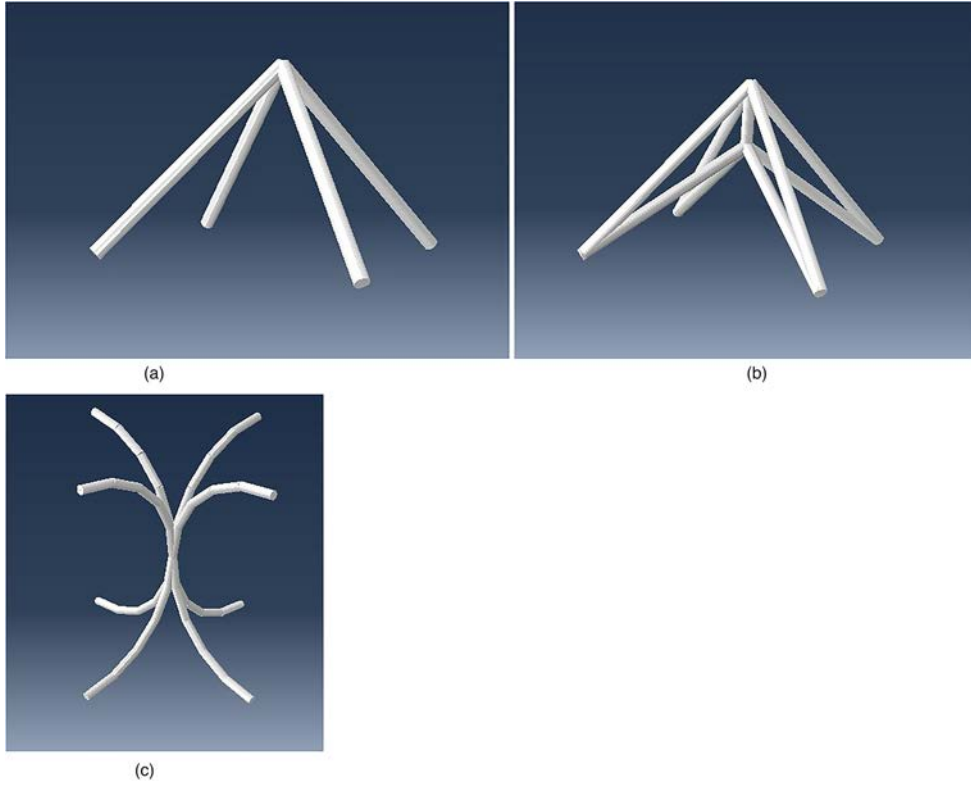


**Figure 10.** (a) Classical PC model, (b) RPC model, and (c) C-HCC model.  
PC: pyramid cell; RPC: reinforced pyramid cell; HCC: half circle cell.

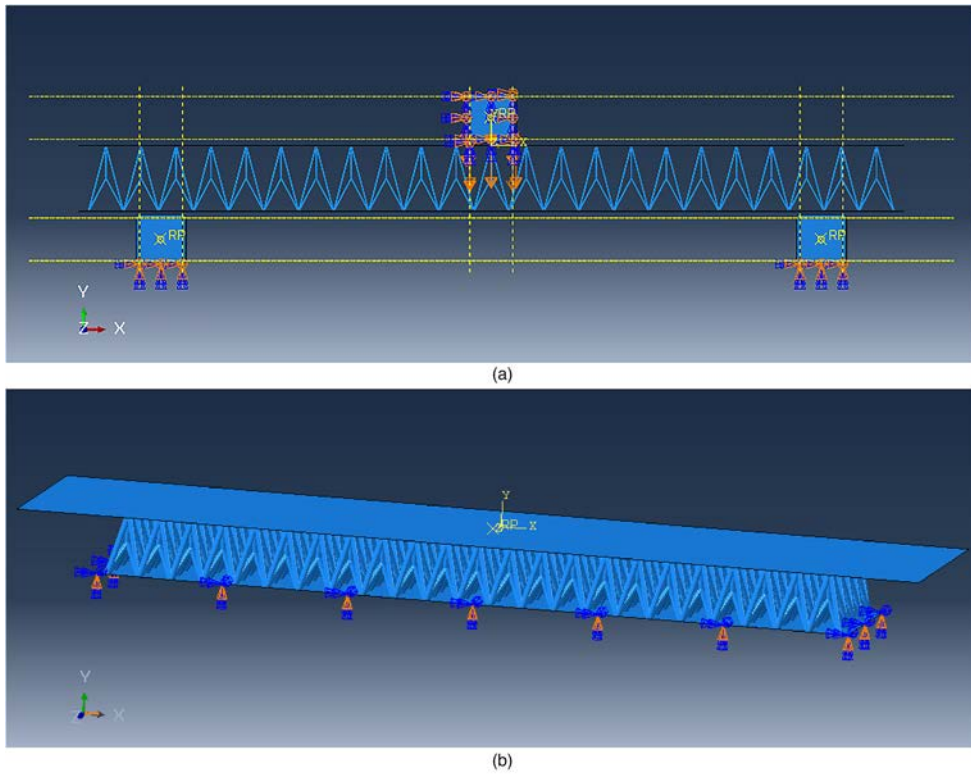
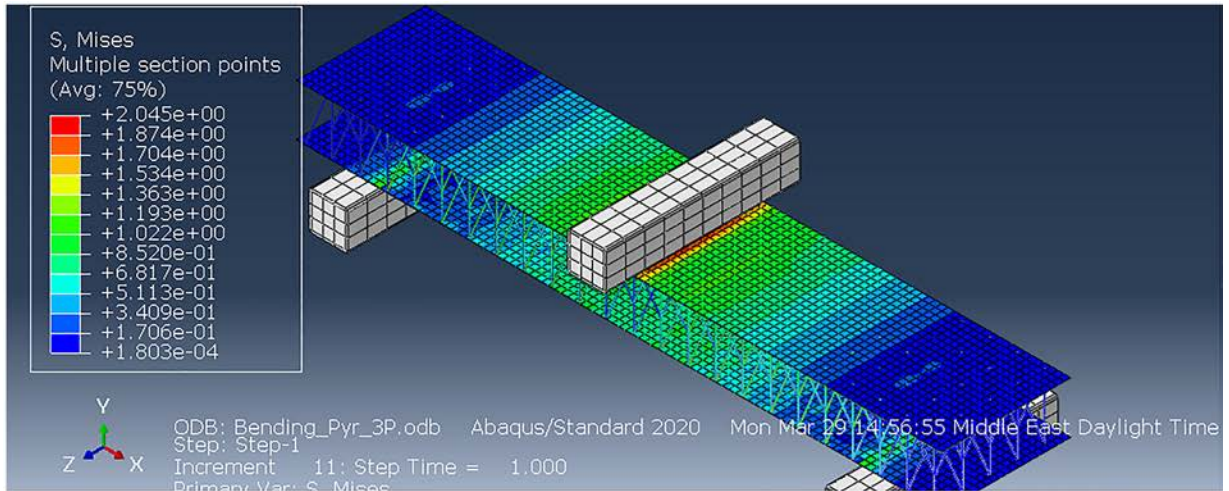
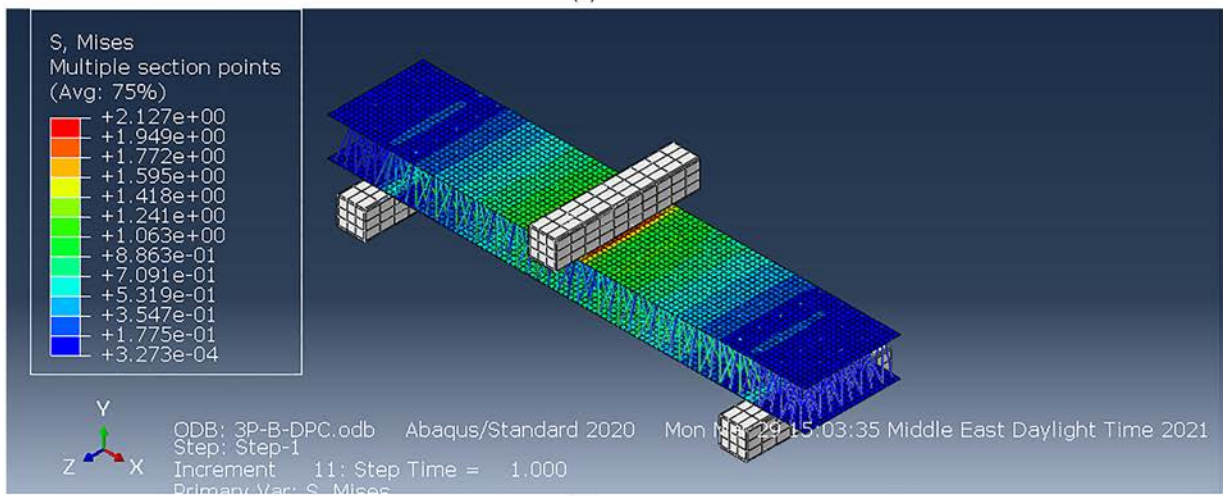


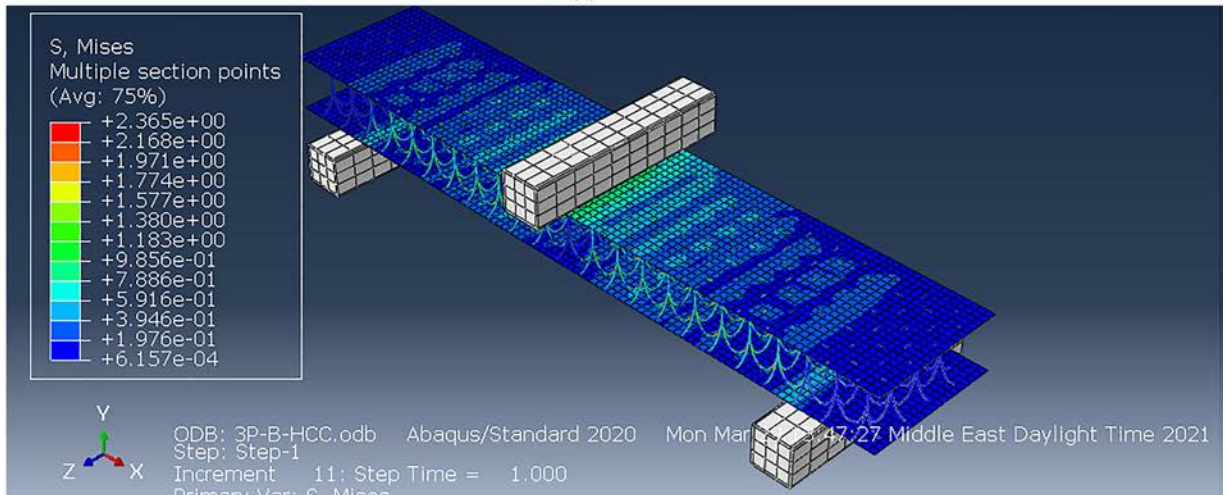
**Figure 11.** Boundary condition and predefined field for a motion for reinforced pyramid cell (RPC).



(a)



(b)



(c)

**Figure 12.** Stress distribution of the panels which is mostly distributed in the skins: (a) PC, (b) RPC, and (c) HCC. PC: pyramid cell; RPC: reinforced pyramid cell; HCC: half circle cell.

lower skin so the fixed as shown in Figure 5. In the simulation, the rigid block is set to move 1 mm into the panel, and then check the maximum reaction of the block and the effect on the skins from the core (Figures 10 and 11).

A second numerical simulation for the three sandwich panels is done to check the resistance of the compression load for each core. The compression tools are assumed as rigid shells. The skins are modeled as shells and the rods

**Table 3.** The bending results of the three-core simulation for max stress, reaction force, skin deformation, and the weight of each.

Type	Max skin stress (MPa)	Reaction forces (N)	Upper skin displacement (mm)
PC	2.04	169	0.0116
HCC	1.57	67	0.0099
RPC	2.11	180	0.0106

PC: pyramid cell; RPC: reinforced pyramid cell; HCC: half circle cell.

**Table 4.** Improvement or weakness of properties for the all-new three cores in accordance with the pyramid core PC.

Type	HCC	RPC
Max skin stress (%)	23.0	−3.4
Reaction forces (%)	−60.3	6.5
Upper skin displacement (%)	14.6	8.6

PC: pyramid cell; RPC: reinforced pyramid cell; HCC: half circle cell.

of the shapes are modeled as wires. The skin and the shaped rod are assembled in the drawing, and the core is attached as a “tie constraint” with the upper and lower skin. The mesh of the rod is set to be 1 mm elements and type of “A 2-node linear beam in space.” For the skin, as a shell, the size of the element is also taken as 5 mm×5 mm, and the type “S4R-A 4-node doubly curved thin shell, reduced integration, hourglass control, finite membrane strains.” The compression tool is a rigid shell with a ref point and the size of the element is 3 mm×3 mm, and the type “R3D4: A 4-node 3-D bilinear rigid quadrilateral.”

The boundary condition for the system is given that the bottom shell is fixed in the depth direction and all rotational axes and free in the horizontal directions. In the simulation, the rigid shell is set to move 2 mm into the panel, and then check the maximum reaction of the shell and the effect on the skins from the core.

## Results and discussions

The results of the experimental tests, simulation, and analytical results of the bending experiment for the sandwich

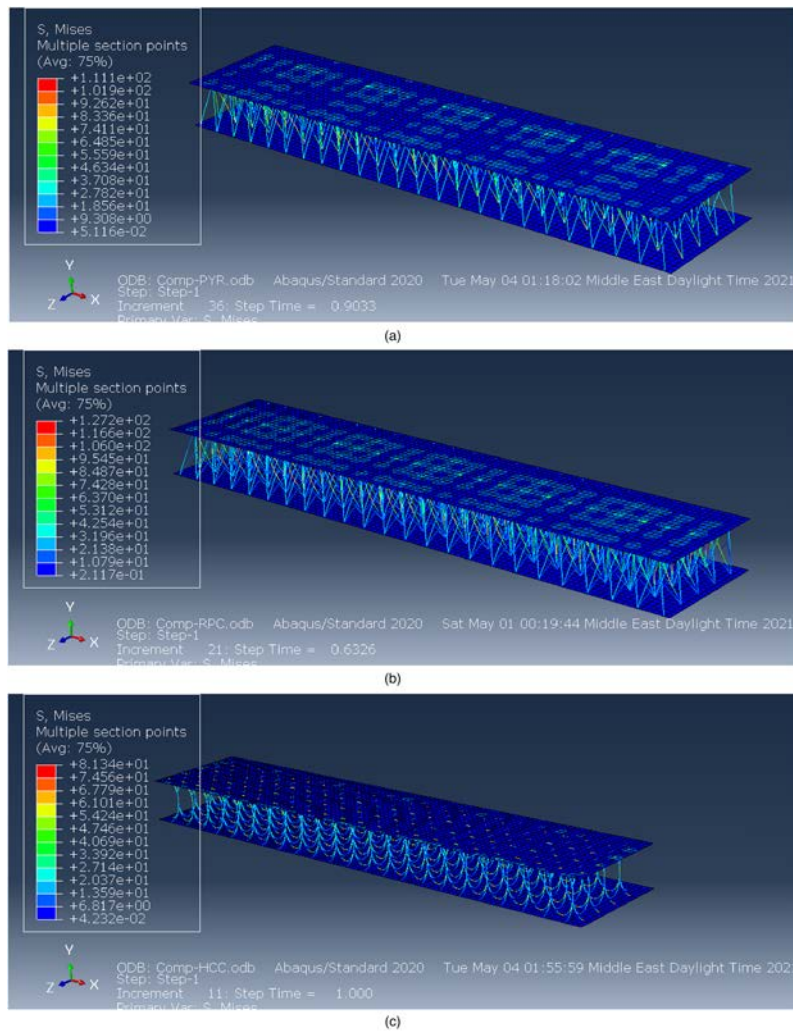


**Figure 13.** Stress distribution for the three panels: (a) PC, (b) RPC, and (c) HCC. PC: pyramid cell; RPC: reinforced pyramid cell; HCC: half circle cell.



**Table 5.** Compression resistance results.

Type	Max skin stress (MPa)	Reaction forces (kN)
PC	41.0	167
HCC	16.3	64
RPC	51.0	225

PC: pyramid cell; RPC: reinforced pyramid cell; HCC: half circle cell.

**Table 6.** Compression resistance percentage comparison.

Type	HCC	RPC
Max skin stress (%)	60.2	24.4
Reaction forces (%)	-61.7	58.0

RPC: reinforced pyramid cell; HCC: half circle cell.

panel for each of the three cores are obtained. The experimental results and the analytical results of the pyramid core are compared to the simulation on ABAQUS with an error of  $< 10\%$ . This verification allows us to consider the simulation results verified of the other shapes since they have similar patterns and types of materials and rods.

Figure 12(a) to (c) shows the Von Mises stress distribution of the three of types panels [a] for “PC,” [b] for “RPC,” and [c] for “HCC” cores. The results of the panels include that the higher the reaction force of the bending tool results the higher the bending resistance of the panel. The same applied to the compression test, the higher the force the higher the resistance of compression. Also, the core of each panel will affect the other skin of the panel by its energy absorption of the applied force, the more the core is stiff, the more the skin will deform and be effected. In the tests done, the deformation of the lower skin, which is the other part of the force, is higher in the “PC” and “RPC” cores than the “HCC” core, which means that the structure of the last one absorbs energy and reaction more the others.

Tables 3 and 4 show the results of the panels for the three cores types. Table 3 shows the results for each core, as the highest resistance to compression, and the HCC is the least resistant. However, HCC also absorbs the most energy and it is the least transfer for the reaction into the plane direction (perpendicular to the reaction force), instead, the DPC, RPC, and PC are almost the same that transfer the reaction to the perpendicular plane.

The second simulation is the compression test of the three panels. Figure 13 shows the Mises stresses distribution of the three types of panels. The same properties as the bending test, the higher the stiffness the higher the deformation and influence of the lower skin of the panel. In the results of the simulations, the “RPC” has the higher compression resistance of the applied force with the higher deformation of the lower skins (Table 5). On the other hand, the “HCC” has the most compression displacement with the lowest deformation of the skins. The results of the reaction of compression test that RPC has 58% higher resistance to compression

in contrast to pyramid core and HCC is less than about 61.7% (Table 6).

## Conclusion

A three-lattice cell sandwich panel was studied in this paper for bending and compression resistance. The first step was to verify the simulation tool by analytical and experimental test of the pyramid core-shaped sandwich panel structure. There was a satisfying percentage of variance of  $< 10\%$  between experimental and simulation tests of the panel which implies to proceed the simulation with ABAQUS for the other cores. The simulation study was done as a bending test and compression test of each panel with the three cores to get 1 mm after that it gets out of the elastic region of the material as shown in the experimental results. For the tree core of the sandwich panel, the deflection is all in the elastic region. The results of the reaction of compression test that RPC has 58% higher resistance to compression in comparison to pyramid core and HCC is less than about 61.7%. And for bending resistance the reactions are both less than 60.3% for the HCC and the RPC is almost the same. Also, the result of the deformation in the skin is 60.2% lower in the HCC core which is the difference between the upper and lower skin. There is a good solution for the energy absorption panel. In the conclusion, the most resistant core for the bending was the PC with about the lowest weight. But the least core that affects the lower skin is the HCC core which absorbed the energy of the applied force and is used as insulation in protection in construction. The RPC is the higher resistance in the compression test which has more application as a stiff slab or a panel which is a pattern needed in the construction to resist compression.


## Declaration of conflicting interests

The authors declared no potential conflicts of interest with respect to the research, authorship, and/or publication of this article.

## Funding

The authors received no financial support for the research, authorship, and/or publication of this article.

## ORCID iD

Khaled Khalil  <https://orcid.org/0000-0002-2044-4798>

## References

1. Ehsan Moosavimehr S and Srikantha Phani A. Sound transmission loss characteristics of sandwich panels with a truss lattice core. *J Acoust Soc Am* 2017; 141: 2921–2932.
2. Wang D-W, Ma L and Wen Z-H. Sound transmission through a sandwich structure with two-layered pyramidal core and cavity absorption. *J Sound Vib* 2019; 459: 114853.
3. Arunkumar MP, Pitchaimani J and Gangadharan KV. Bending and free vibration analysis of foam-filled truss core sandwich panel. *J Sandwich Struct Mater* 2018; 20: 617–638.

4. Lukin AA, et al. Beams with corrugated web: calculation peculiarities of bending torsion analysis. *Procedia Eng* 2016; 153: 414–418.
5. Monteiro JG, et al. Evaluation of the effect of core lattice topology on the properties of sandwich panels produced by additive manufacturing. *Proc Inst Mech Eng, Part L: J Mater: Design Appl* 2021; 235: 1312–1324.
6. Tao W and Leu MC. Design of lattice structure for additive manufacturing. In: International symposium on flexible automation (ISFA), 2016. IEEE, pp. 325–332
7. <https://www.matweb.com/search/DataSheet.aspx?MatGUID=eb7a78f5948d481c9493a67f0d089646> (2020)
8. Valdevit L, Hutchinson JW and Evans AG. Structurally optimized sandwich panels with prismatic cores. *Int J Solids Struct* 2004; 41: 5105–5124.
9. Chen Z, et al. Novel negative Poisson's ratio lattice structures with enhanced stiffness and energy absorption capacity. *Materials (Basel)* 2018; 11: 1095.
10. Bagheri A, et al. Determination of the elasticity modulus of 3D-printed octet-truss structures for use in porous \_prosthesis implants. *Materials (Basel)* 2018; 11: 2420–2436.
11. Liu T, Deng ZC and Lu TJ. Design optimization of truss-cored sandwiches with homogenization. *Int J Solids Struct* 2006; 43: 7891–7918.
12. Liu T, Deng ZC and Lu TJ. Structural modeling of sandwich structures with lightweight cellular cores. *Acta Mech Sin* 2007; 23: 545–559.
13. Ptochos E and Labeas G. Elastic modulus and Poisson's ratio determination of micro-lattice cellular structures by analytical, numerical and homogenisation methods. *J Sandwich Struct Mater* 2012; 14: 597–626.